The effects of a hydrogen-rich ground cover on cosmogenic thermal neutrons

The effects of a hydrogen-rich ground cover on cosmogenic thermal neutrons: implications for exposure dating

T. J. Dunai*, S. A. Binnie, A. S. Hein and S. M. Paling

*Corresponding Author

The effects of a hydrogen-rich ground cover on cosmogenic thermal neutrons: implications for exposure dating

T.J. Dunai[1,2]* , S.A. Binnie[1,2], A. Hein[1], S.M. Paling[3]

[1] School of Geosciences, University of Edinburgh, Drummond Street, Edinburgh EH8 9XP, UK

[2]Institut für Geologie und Mineralogie, Universität zu Köln, Greinstraße 4, Gebäude 902, 50939 Köln, Germany

[3] Department of Physics and Astronomy, Hicks Building, Hounsfield Road, Sheffield S3 7RH, UK

*corresponding author

We present results of thermal neutron flux measurements in experimental granite piles that were tailored to study the effect of hydrogen-rich covers on that flux. We find that hydrogen-rich covers (polyethylene, water), used as proxies for snow, dead and/or live plant matter, increase the thermal neutron flux in an underlying rock surface significantly, as compared to the state without cover. The rock serves as the main source for thermal neutrons, the hydrogen-rich cover as a neutron reflector. In situations where the thickness of such a cover would be negligible in terms of high-energy neutron (>10 MeV) attenuation, e.g. 2-3 cm water equivalent cover, a significant enhancement of the thermal neutron flux (factor >2.5±0.5) can be achieved. This increase is made up of three components (Masarik et al., 2007): (1) reflected thermal neutrons (albedo neutrons), (2) moderated fast neutrons from the ground, and (3) moderated fast neutrons from the atmospheric cascade (Masarik et al., 2007). The higher thermal neutron flux increases the production rates of those cosmogenic nuclides that have a significant thermal neutron production pathway (^{3}He, ^{36}Cl, ^{41}Ca). Ignoring this effect in situations where target nuclei (^{6}Li, ^{35}Cl, ^{40}Ca) are abundant will severely underestimate production rates. The effect of hydrogen-rich ground cover on the thermal neutron flux has the potential to be used for studies that are aimed at reconstructing the persistence of past plant/snow cover. Isotopic ratios of spallogenic versus predominantly thermal neutron produced nuclides, would reveal the presence or absence of hydrogen-rich cover in the past as compared to the present-day situation.

Keywords: cosmogenic nuclide; neutron flux; snow cover; plant cover; production rate

1. Introduction

The energy spectrum of the secondary neutrons of the cosmic ray cascade is in equilibrium from a few hundred metres above the Earth's surface to several kilometres in the atmosphere, i.e. the neutron energy spectrum remains essentially unchanged (Goldhagen et al., 2003; Goldhagen et al., 2002; Kowatari et al., 2005; Lal and Peters, 1967). However, near the Earth's surface both neutron production and scattering properties change profoundly, leading to a non-equilibrium situation (Hendrick and Edge, 1966; Kastner et al., 1970; Kodama, 1983; Masarik et al., 2007; O'Brien et al., 1978). In particular, the flux of thermal neutrons increases dramatically, by approximately one order of magnitude, due to increased production in the solid Earth and effective moderation by water/moisture at the ground level (Hendrick and Edge, 1966; Kastner et al., 1970; Kodama, 1983; Masarik et al., 2007; O'Brien et al., 1978). This perturbation of the thermal neutron flux is measurable up to 100 m above ground (Hendrick and Edge, 1966); the attenuation of this perturbation occurs due to the large reaction cross section of ^{14}N for thermal neutrons and the high abundance of nitrogen in air (Hendrick and Edge, 1966). Over the length-scale of 100 m, the atmosphere (at sea level) can be considered as an effective sink for thermal neutrons emanating from the Earth's surface.

The increased thermal neutron flux above the Earth's surface derives from secondary neutrons that are produced and moderated in the uppermost ~50 g/cm^2 in the ground and then 'leak' back into the atmosphere (Masarik et al., 2007; O'Brien et al., 1978; Phillips et al., 2001). The scattering of neutrons by protons (hydrogen nuclei) is a particularly effective way by which higher energy level neutrons are moderated to thermal neutrons (Reuss, 2008). As a source of hydrogen nuclei the water content of rocks or soils is, therefore, a crucial parameter for determining the thermal neutron flux near the ground/air interface (Phillips et al., 2001). Once 'thermal', neutrons are in energy equilibrium with their surroundings; they are equally likely to become accelerated or decelerated in response to collisions with other nuclei (Reuss, 2008) and the resulting direction of movement is random (Phillips et al., 2001). The attenuation of the thermal neutron flux in rocks/soils occurs due to neutron capture reactions by elements that constitute the rock/soil matrix (Phillips et al., 2001). These neutron capture reactions may produce cosmogenic nuclides used in Earth science applications. Cosmogenic nuclides with significant production by thermal neutrons are ^3He, ^{36}Cl and ^{41}Ca; they are produced by neutron capture by ^6Li, ^{35}Cl and ^{40}Ca, respectively (Audi et al., 2003; Dunai, 2010; Dunai et al., 2007; Liu et al., 1994; Nishiizumi et al., 2000).

Any hydrogen-rich layer (e.g. snow, ice, plant matter) covering a neutron source (e.g. rock or soil) can effectively reflect thermal neutrons back into the source, i.e. it has a large albedo for emitted thermal neutrons. For example, a thick (> ~6-8 cm) water layer will reflect 80% of incoming thermal neutrons back into their source (Reuss, 2008). The efficiency of natural neutron reflectors is largely governed by their hydrogen concentration and neutron absorption properties (Csikai and Buczkó, 1998; Király and Csikai, 2000; Reuss, 2008). Furthermore, a hydrogen-rich layer on the ground may increase the thermal neutron flux beneath by returning fast neutrons (e.g. neutrons from evaporation reactions in the ground, 1-10 MeV) moderated to thermal energies, which may otherwise leak to the atmosphere (Kodama, 1983; Masarik et al., 2007). Also incoming secondary neutrons from the atmospheric cascade will be moderated by a hydrogen-rich layer and increase the thermal neutron flux beneath it (Masarik et al., 2007). The increase of the thermal neutron flux in the ground near the ground/air interface, by a hydrogen-rich layer at that interface, is therefore made up of three components (Masarik et al., 2007): (1) reflected thermal neutrons, (2) moderated fast neutrons from the ground, and (3) moderated fast neutrons from the atmospheric cascade (Masarik et al., 2007). Conversely, the thermal neutron flux in the ground may be reduced to some extent by hydrogen-rich layers which shield the ground from incoming cosmic rays (Hatton and Carmichael, 1964).

The effect of hydrogen-rich layers on the cosmogenic thermal neutron flux in solids has been experimentally determined (neutron source: lead; moderator/reflector: polyethylene; Hatton and Carmichael 1966) and numerically modelled (neutron source: average terrestrial body; moderator/reflector: water; Masarik et al. 2007). These results indicate that there is a potentially large (1.3 – 4 fold) increase in the thermal neutron flux (Hatton and Carmichael, 1964; Masarik et al., 2007), with only thin covers of neutron reflectors (Hatton and Carmichael, 1964). Such an enhanced thermal neutron flux will necessarily increase cosmogenic production of nuclides with a significant thermal neutron capture pathway. These studies (Hatton and Carmichael, 1964; Masarik et al., 2007) demonstrate that the regular approach of considering any mass-cover (of hydrogen-rich or not) as an attenuator of the cosmic ray flux, as commonly undertaken for exposure dating (cf. Gosse and Phillips 2001) is probably incorrect for nuclides with a significant thermal neutron capture production pathway (^{3}He, ^{36}Cl and ^{41}Ca) and a hydrogen-rich ground cover (snow, ice, plant matter, moist soil). While the previous studies (Hatton and Carmichael, 1964; Masarik et al., 2007) clearly show the importance of hydrogen-rich cover, the translation for the use in applications of in-situ produced cosmogenic nuclides remains difficult. The extent to which lead (Hatton and Carmichael, 1964) can be used as proxy for rock is currently unclear, while the numerical calculations of Masarik

et al. (2007) consider only thick (20 cm water) covers and would benefit from experimental verification.

In this study we investigate the effect of a hydrogen-rich cover for rocks of granitic composition. Granitic rocks contain minerals often used for cosmogenic applications, utilizing ^{3}He and ^{36}Cl, and other minerals which show potential for future development utilizing ^{41}Ca (Dunai, 2010; Farley et al., 2006; Gosse and Phillips, 2001). In addition granite contains abundant concentrations of target nuclides (^{6}Li, ^{35}Cl and ^{40}Ca) with significant thermal neutron capture cross-sections producing these cosmogenic nuclides. Our experimental results confirm the magnitude of effects described by Hatton and Carmichael (1966) and Masarik et al. (2007), and demonstrate their importance for common situations encountered in applications of in-situ produced cosmogenic nuclides to Earth sciences.

2. Methods and experimental setting

We measured the thermal neutron flux in two identical granite piles. One pile was used to monitor changes in the cosmic ray flux and the environmental neutron field (Kodama, 1983; Zreda et al., 2008), the other was modified by placing polyethylene, water (of various thickness) and/or further granite on top. Thus, in response to these modifications, the relative changes in thermal neutron flux rates, corrected for external flux variations, were obtained. The basic dimensions of both granite piles were 120 x 130 x 60 cm (Fig. 1), the piles were built from individual granite blocks, each 5 x 10 x 20 cm. They were exposed at 198 m elevation on the Ministry of Defence's (MOD's) Kirknewton Airfield, Scotland, UK (Fig. 2). The dimensions of the granite piles were chosen so that the lateral distance from the neutron counting tubes to the outer surface of the sides of the piles was at least six times the average thermal neutron diffusion length (23 g/cm^{2} (Liu et al., 1994); equating to ~9 cm in granite with a measured density of 2.64 g/cm^{3}; see also Fig. 1). This meant that the lateral loss of thermal neutrons from the sides of the piles would be insignificant at the position of the counter tubes (less than 5% are lost beyond 3 diffusion pathlengths; Fig. 1). Due to practical and financial considerations we did not build a larger granite pile of the dimensions comparable to the concrete pile used by Liu et al. (1994); however, we note that the dimensions of the piles used are not unlike those of commonly sampled features for exposure dating (e.g. moraine boulders). The composition of the granite is provided in Table 1.

The ^{3}He proportional counting tubes (Centronic 25He3/304/25 tubes; 25 mm diameter aluminium tubes, 4 bar filling pressure) were inserted into 3 cm diameter holes drilled horizontally into the top layer of granite blocks (Fig. 2). The centre of these holes was 2.5 cm below the surface. To protect the counting tubes from moisture they were placed inside the inner tubes of bicycle tyres (0.5 mm thick, Isoprene), with 5 g zeolite desiccators placed at each end of the tubes. Both pile assemblies were housed in individual aluminium frames (150 x 150 x 100 cm) that were covered on five sides (not the bottom) with 0.5 mm thick corrugated PVC. As hydrogen-rich material we used sheets (100 x 100 cm) of high-density polyethylene (HDPE, 0.941 g/cm^{3}) of 0.3, 0.5 and 1 cm thickness. For the water-experiments, water was placed inside a basin (100 x 100 x 30 cm) built from extruded (hollow) Al-struts (3 x 3 cm; Bosch-Rexroth) that supported HDPE sheets (3 mm thick). A 0.3 mm low density PE sheet waterproofed the basin which was placed on top of the piles (Fig. 2).

The ^{3}He neutron counting tubes were calibrated at the National Physical Laboratory at Teddington, UK. The two tubes had identical cross-sections of 28.84±0.48 cm^{2} (tube # 0844-345) and 29.35±0.46 cm^{2} (tube # 0844-346) (±2σ) for sub-cadmium-cut-off neutrons (Westcott fluence; (Thomas and Kolokowski, 2005)). Ludlum 2350-1 data loggers were used to collect data during the field experiments.

Background measurements were conducted at the Boulby Underground Science Facility, located at >1100m depth, in a working potash and salt mine on the North East coast of England (http://www.stfc.ac.uk/Sites+and+Facilities/38100.aspx). The background counting rates of bare ^{3}He counting tubes inserted into the same granite blocks used in the surface experiment and surrounded by > 30 cm Polypropylene pellets (>20 cm solid PP equivalent) were determined. The background was found to be partly due to noise in one of the Ludlum data loggers. Voltage settings were adjusted in both loggers, which reduced noise in the affected logger (to 0.005 Hz, this logger was later used with pile 1) and the sensitivity of both logger/counter assemblies to 15% below the maximum attainable neutron counting rate (verified using a ^{252}Cf neutron source). The background tube counting rates after the adjustments was 0.0038±0.0004 Hz (± Poisson). Subsequent measurements were corrected for this background.

Typical counting rates obtained with bare ^{3}He counters in the unmodified granite piles exposed on the airfield were 0.05 Hz (±1.6% Poisson; ~20 hour integration times; data of pile 1). Day to day variations, due to changes in environmental conditions (see below) and/or cosmic ray flux were ±10% (±1 σ). To eliminate the effects of this variability from our measurements we normalized the counts logged in pile 2 to the mean of the counts obtained for the control pile 1. That is, for the

integrated duration of each experiment the absolute amount by which the counts in pile 1 were above or below the mean was used to correct the counts in pile 2. Normalized count rates of repeat measurements (n=5) of the thermal neutron fluxes in pile 2 without cover (i.e. in identical configuration to pile 1) were reproducible to ±3% (±1 σ). The absolute value of that uncertainty, ±0.0015 Hz, is used as estimate for the uncertainty of relative counting rates throughout this study. Due to the already low counting rates with bare ^{3}He counters, no experiments with Cd-shielding were performed. Cd-shielding would have lowered counting rates by a factor of ~0.1 or more (Phillips et al., 2001), close to the background rates of our experimental setup at low altitude. By not conducting Cd-shielded experiments, filtering the results to obtain a pure thermal neutron signal is not possible. The maximum contribution of epithermal neutrons to the absolute count rate in ^{3}He counters in experimental settings such as ours is ~10% (Phillips et al., 2001). This contribution will reduce any relative changes in neutron counting rates between piles 1 and 2 in the experiments with hydrogen-rich cover because the leakage/reflection is more important for thermal neutrons than for epithermal neutrons (for the relative importance of leakage see Phillips et al. 2001). However, this reduction probably remains within the uncertainties of our experimental setup.

The moisture in the pasture adjacent to the granite piles changed from above wilting point to water-logged during the experiments, conducted between May and September 2009. The location of the airfield is called 'Whitemoss' (moss: bog, swamp; a fen, morass in Scotland; Oxford English Dictionary Online). The tarmac runway on which the granite piles were erected was covered by continuous vegetation (moss, grass; the runway has been out of use for 20 years), which was cleared at the sites of the piles, but was left undisturbed elsewhere. The composition of the tarmac is provided in Table 1. The changes in environmental conditions (moisture levels), which will influence the local neutron fluxes (Kodama, 1980; Kodama et al., 1985; Zreda et al., 2008), are cancelled out by normalizing the count-rates obtained in the modified pile (2) with the count rates of the control pile (1). Both granite piles had identical distance to the adjacent pastures (Fig. 2), were situated on the same tarmac of constant thickness (30±5 cm; measured by drilling), and the type and density vegetation on the tarmac was indistinguishable at both sites. Considering the large footprint of environmental neutrons (Zreda et al., 2008) it is improbable that the environmental neutron flux was significantly different at the sites of the two piles at any time.

As mentioned above, both HDPE sheets and water were used as hydrogen-rich covers on pile 2. HDPE sheets were used for thin layers (0.3 – 2 cm), water for larger thicknesses (2.5 – 25 cm). This approach was chosen to avoid inaccuracies arising from unevenness or tilt of the pile's surface on an overlying water layer, and due to evaporation during the experiment (the latter would be relatively

more important in experiments with a thin water cover). Evaporation losses in the water experiments were monitored by measurements of water depth at the onset and the end of the experiments; the corresponding means are used in tables and figures and the measured depth range used as uncertainty (typically ±0.5 cm). Considering the density of the HDPE used (0.941 g/cm^3) and the relative hydrogen concentration in polyethylene and water it can be calculated that a cover of 1 cm of HDPE has an equivalent effect to thermal neutrons as a cover of 1.21 cm water (Király and Csikai, 2000). All cover thicknesses were translated into water equivalent cover and in the case of the water experiments the effect of the 0.3 cm HDPE lining sheet in the basin (see above) was considered accordingly.

The HDPE sheets and water cover were placed directly on top of the granite, centred on the pile's surface (Fig. 1). In one experiment we repeated a 2 cm HDPE cover, with air-gaps between HDPE sheets, to mimic situations where the neutron reflector/moderator is porous (e.g. snow). Granite shielding experiments were conducted with 1 and 2 cm HDPE, and without cover to study the effects of hydrogen-rich ground cover on the thermal neutron flux in the subsurface (0-30 cm granite or 0-79 g/cm^2 shielding; in 5 cm granite increments). The granite blocks used for these shielding experiments were identical to those used to construct the piles. In further experiments we displaced the counting tube of pile 2 laterally (eastwards), to verify the effects of lateral diffusive loss of thermal neutrons from the pile. These experiments were conducted both with and without a 2 cm HDPE cover. In experiments with an HDPE cover, the sheet was flush with the eastern edge of the pile (instead of being centred, i.e. 10 cm from the pile's eastern edge).

It is important to note that our experiments used bare ^{3}He counters (as did Liu et al. 1994), whereas previous experimental studies of environmental neutrons aimed at the effect of water/moisture at the ground/air interface used ^{3}He or BF_3 counters surrounded by a 2-2.5 cm Polyethylene moderator (Kodama, 1980; Kodama et al., 1985; Zreda et al., 2008). Such moderated counters have an almost constant response to neutrons in the energy range of 1eV-1MeV (Kodama et al., 1985; Yamashita et al., 1966) and suppress incoming thermal neutrons (diffusion length of thermal neutrons in polyethylene is 2.5 cm; Hatton and Carmichael 1966), whereas, bare ^{3}He neutron detectors are mostly sensitive to thermal neutrons (~0.025 eV) and have a steeply declining response to higher energies (Goldhagen et al., 2003; Vega-Carillo et al., 2005). The moderators on neutron monitors used in other studies (Kodama, 1980; Kodama et al., 1985; Zreda et al., 2008) remove most effects specific to the thermal neutrons we measured here. Thus, we stress that our results are not directly comparable to other studies (Kodama, 1980; Kodama et al., 1985; Zreda et al., 2008), which have

had different scientific goals and applications, without accounting for the differences in the response function of the detectors.

3. Results

Results of three experiments, in which we investigated (i) the effect of lateral displacement of the neutron detectors; (ii) the effect of adding granite above the neutron detectors (mimicking a depth-profile); and (iii) the effect of applying neutron reflectors of varying thicknesses, are presented below.

3.1. Neutron diffusion profiles

The neutron detector tube in pile 2 was displaced in 10 cm increments from the central position towards the edge of the pile (Fig. 1). We performed these experiments with and without neutron reflector. In the experiments without reflector the count rates begin to drop when the neutron detector was less than 30 cm from the edge of the pile and the drop appears to be linear (Fig. 3). At 10 cm from the edge, the measured count rate is approximately two thirds of the count rate at the central position (Fig. 3). Extrapolated to the edge of the pile, the count rate is, within uncertainties, half of the count rate at the central position. This behaviour is as expected considering the loss of thermal neutrons to the atmosphere from the side of the pile and the ~9 cm thermal neutron diffusion length in granite (see above). These data confirm that the bulk of the thermal neutrons are produced within the pile and that the thermal neutrons from the environment surrounding the pile do not contribute significantly to the flux within the piles.

The neutron count rates in the experiments with neutron reflector (2 cm HDPE) are ~2.4 times higher than the corresponding experiments without reflector (Fig. 3), showing a drop of count rates from the centre to the near-edge position. Within 30 cm of the edge of the pile the trend of the count rates is parallel to that of the corresponding experiments without a reflector. However, unlike the previous experiments (no reflector) count rates continue to increase towards the centre of the pile (40-60 cm from the edge), although at a lower rate than closer to the edge (0-30 cm). This pattern can be explained by the combined effect of: 1. thermal neutron loss; 2. loss of lateral contribution of fast neutrons (1-10 MeV) from evaporation reactions, and 3. the finite dimensions of the experimental pile. The neutrons from evaporation reactions have a much larger attenuation length than the diffusion lengths of thermal neutrons (~150-180 g/cm^2, or 57-68 cm as compared to 24 g/cm^2 or 9 cm in granite of 2.64 g/cm^3 (Gosse and Phillips, 2001, Liu et al., 1994). Edge effects

will, therefore, reach further into the pile in experiments with reflectors as is explained in the following.

A neutron counting tube beneath a theoretical infinite surface that is covered by a reflector could receive fast neutrons from laterally distant sources. Without a reflector these fast neutrons could leave the surface/atmosphere interface at a shallow angle to the interface (Fig. 4), with a neutron reflector these neutrons could be scattered back into the surface. These reflected fast neutrons, once thermalized, would be recorded by the neutron counting tube. A neutron counting tube at the lateral edge of a semi-infinite surface with a corresponding reflector, would only receive 50% of those thermalized evaporation neutrons as compared to an infinite surface. Three attenuation lengths from the edge, the reduction of neutrons would mean a less than 5% drop of the total count rate. This is similar to the situation described above for the edge effects that reduce thermal neutrons; however, there it was a loss *from* the neutron source, whereas here it is the loss *of* a neutron source. Applying these considerations to the actual pile, the edge effects would be significant (>5%) three fast neutron attenuation path-lengths from the edge, a distance exceeding the dimensions of the pile (Fig. 1). This is in line with the observation that the diffusion profile with a reflector (Fig. 3) does not reach a plateau that is free of edge effects, as was achieved for the experiments without reflector. Considering that at the pile-edge position both effects (loss of thermal neutrons and loss of source of evaporation neutrons) leads to a 50% drop of the corresponding counting rate as compared to the plateau value, it can be estimated that the expected plateau count rate of the reflector experiments is about 35% higher than measured at the centre of the actual pile. Consequently the count rates on the anticipated plateau of the reflector experiment are about 3.3 times higher than the plateau of the experiment without reflector. This is a conservative estimate because counting rate at the edge position is affected (lowered) by the finite dimensions of the granite pile. That is, the counting rates would be higher if the eastern edge would receive fast neutrons from regions beyond the northern, southern and western edge of the pile these edges are between one to two fast-neutron attenuation lengths away from the eastern edge position (Fig. 1). For the above consideration of the actual pile it is important to keep in mind that due to the wet surroundings of the piles (see sect. 2), the majority of fast neutrons that are produced in the soils in line of sight surrounding the piles are moderated to lower energies before they leave the ground. Thus the fields surrounding the piles cannot replace the ‘missing’ rock of the finite piles in terms of fast neutron flux.

3.2. Depth profiles

In order to mimic a depth profile, pile 2 was modified by adding additional layers of granite on the top in 5 cm increments up to a total additional thickness of 30 cm (Fig. 1). In the experiments without a neutron reflector on top of the thus modified pile the thermal neutron flux increases with depth until 20 cm before levelling off, possibly then declining at 30 cm (Fig. 5). This behaviour is in agreement with model calculations (Phillips et al., 2001; Schimmelpfennig et al., 2009) and measurements (Liu et al., 1994) that predict that the thermal neutron flux in granite increases with depth, reaching a maximum at between ~20-25 cm and declining at depths > 30 cm (Fig. 5). The initial increase in the thermal neutron flux is due to the decreasing fraction of neutrons lost to the atmosphere with depth below the surface/atmosphere interface (Phillips et al., 2001). That the results of model calculations (Phillips and Plummer, 1996; Schimmelpfennig et al., 2009) do not accurately agree with our experimental results is probably, at least partially, due to the finite dimensions of the experimental pile used (see discussion above, Section 3.1.), whereas the concepts of the model calculations (Phillips and Plummer, 1996; Schimmelpfennig et al., 2009) implicitly assume an infinite surface. For the purpose of this study it should suffice to note that the subsurface thermal neutron flux qualitatively behaves as predicted.

In additional experiments we placed 1 cm and 2 cm HDPE sheets on top of the depth profile. With 1 cm HDPE cover the thermal neutron flux increases with depth, similarly to the fluxes measured without cover except the surface flux is increased by ~50% (Fig. 5). At ~20 cm depth the thermal neutron flux is indistinguishable within uncertainties from the situation without neutron reflector. With 2 cm HDPE cover the situation is reversed, i.e. the thermal neutron flux at the surface is increased by a factor of ~2.4, decreasing to a normal flux (i.e. that without cover) at a depth of 25 cm. In line with the nature of diffusive thermal neutron transport, the disturbance of the thermal neutron flux by a neutron reflector on top of the neutron source (the granite) does not reach depths greater than 3 multiples of the diffusion length of thermal neutrons (Reuss, 2008).

3.3. Effect of neutron reflectors of varying thickness and density

The experiments in which neutron reflectors (HDPE, water) of varying thickness (0-25 cm, water equivalent) are applied show a pronounced increase of the neutron counting rate (Fig. 6). This increase is significant (>10%) even at low reflector thicknesses (6 mm), and reaches a maximum between 2.4 and 5.8 cm water equivalent cover. The maximum count rates are 2.4 times higher than in situations without a neutron reflector (Fig. 6). With larger reflector thicknesses the counting rate decreases due to the mass-attenuation of the incoming high-energy cosmic ray flux by the reflector

(Hatton and Carmichael, 1964). The general shape of the response curve obtained (Fig. 6) is very similar to the neutron monitor experiments of Hatton and Carmichael (1964), indicating that there is no requirement to invoke different processes for our granite piles than those operating in the standard MN64 neutron monitor. Quantitative differences are in the neutron-production, moderation and absorption efficiency of lead as compared to granite, and in the dimensions of the pile relative to the attenuation length in lead and granite; which cause the differences in the relative sizes of the maxima (Fig. 6).

The large 4.1 fold increase of flux calculated in the numerical simulations of Masarik et al. (2007; Fig. 6) is partly due to the fact that Masarik et al. (2007) simulated infinite surfaces/reflectors, whereas our pile had finite dimensions. As explained above, an infinite granite pile with reflector would have the thermal neutron flux increased by at least 3.3 fold. Further differences will be due to the different surface composition simulated (average terrestrial composition: 0.2% H, 47.3% O, 2.5% Na, 4.0% Mg, 6.0% Al, 29.0%, Si, 5.0% Ca and 6.0% Fe, all wt%; Masarik et al. 2007) as compared to the composition of the granite used here (Table 1). Considering the compositional differences and the systematic uncertainties of the numerical simulations (10-15%, ±1σ; Masarik et al., 2007), as well as the uncertainty involved in the extrapolation of our experimental results to infinite shapes (minimum estimate, see above), the results of the numerical simulation (Masarik et al., 2007) and our experiment are currently indistinguishable. Considering the effects of finite irradiation geometries, that is a somewhat smaller effect of hydrogen-rich covers for smaller piles (boulders in nature), we estimate that in 'normal' sampling situations for terrestrial cosmogenic studies the maximum increase of the thermal neutron flux at the surface, due to a hydrogen-rich cover, will be in the range of 2.5±0.5 fold. From the results of the above neutron diffusion experiments (sect 3.1.) we estimate that rock surfaces wider than ~50 cm lateral extent, such as on top of a boulder, are capable to support an effect of this size. For smaller rock surfaces the maximum effect of cover is still on the order of a 2.0±0.5 fold increase; hence the effects of hydrogen-rich covers may be reduced but cannot be avoided by sampling smaller features.

In one experiment we added spacers between the HDPE sheets to mimic a porous neutron reflector filled with air (e.g. snow, duff, moss). The configuration was: granite - 1.5 cm gap - 0.5 cm HDPE - 1.5 cm gap - 0.5 cm HDPE - 3.5 cm gap - 1 cm HDPE; resulting in a gap to reflector thickness ratio of 2.7 : 1 (water equivalent). This gap (air) to reflector ratio is equivalent to snow with a density of 0.27 g/cm^3, which is within the typical range for snow (Gosse and Phillips, 2001; Onuchin and Burenina, 1996). We find no resolvable difference between the experiments without and the experiment with the spacer, both situations having the same reflector thickness (Fig. 5). This behaviour is as

expected, based on the long attenuation length for thermal neutrons in air (32 m, at sea level). This long attenuation length arises from the fact that, despite a relatively high attenuation coefficient (3.9 g/cm^2), air has low density (0.0012 g/cm^3 STP). For the purposes of our experiments this means minimal absorption by nitrogen over the gap distances involved.

The indistinguishable effect we obtain for HDPE and water of (2.42 vs. 3.2 cm water equivalent thickness; Fig. 6) confirms that the efficiency of natural neutron reflectors is largely governed by the hydrogen concentration and the neutron absorption properties of the reflector (Csikai and Buczkó, 1998; Király and Csikai, 2000; Reuss, 2008); which is assisted by the similar thermal neutron absorption and reflection properties of carbon and oxygen (Chadwick et al., 2006; Csikai and Buczkó, 1998). Csikai and Buskó (1998) demonstrated this for a wide range of organic and inorganic compounds. Consequently our neutron reflector results, discussed in the following, are equally relevant for both oxygen- and carbon-bearing neutron reflectors (ice, snow, plant matter).

4. Discussion

Our experimental results show first and foremost that a thin hydrogen-rich cover, which would have a negligible effect on the attenuation of high-energy neutrons (> 10 MeV), drastically enhances the thermal neutron flux in the subsurface near the ground/air interface. A 2.5 cm (water equivalent) thick hydrogen-rich ground cover, equating to 7.5-15 cm snow cover (Onuchin and Burenina, 1996), more than doubles the thermal neutron flux at the ground/cover interface. The same groundcover would reduce the high-energy neutron flux by only ~1.5% (Gosse and Phillips, 2001). This increase in thermal neutron flux persists when ground cover becomes thick enough to noticeably attenuate the high-energy neutron flux. Before we discuss the effects on terrestrial cosmogenic nuclide production rates, exposure ages and process rates, we will consider the potential effect of plant matter on the thermal neutron flux in the subsurface.

4.1. Plant cover

The minimum hydrogen content of dead or live plant matter is provided by the hydrogen content of cellulose and/or lignin, which are the major structural and the most decay-resistant components of vascular plants and mosses. Cellulose and/or lignin make up the bulk of dry plant matter (DM), which is considered to be oven dry material. These compounds contain 6.2 wt% (cellulose) and ~6.7 wt% (lignin) hydrogen, compared to the 11.1 wt% hydrogen content of water. The water equivalent of 1 g/cm^2 of dry plant matter, in relation to neutron albedo (Csikai and Buczkó, 1998; Reuss, 2008),

is thus ~0.6 g/cm^2. Any moisture contained in the plant matter increases this value. On the low end of moisture content scale is decaying plant matter in forests (duff), which commonly contains ~40 wt% water (all values for moisture content used here are relative to DM, following Robichaud et al., 2004). However, this is a value that can range widely (0 - >200 wt%) depending on species, site and season (Robichaud et al., 2004) and the likely maximum value in temperate forest is ~260 wt% (Bernard, 1963). Living wood has 60-200 wt% water content, the actual value depends on the location in the tree, the species and the season (Dinwoodie, 2000). Values of around 100±30 wt% appear to apply to many trees in temperate climate zone (Dinwoodie, 2000). Green grass has a moisture content in the order of ~80 wt% (Hooper, 1980). Finally, water content of common mosses at full turgor ranges between 150 and 1100 wt% (3600 rpm centrifuged moss; (Dilks and Proctor, 1979). This, far from exhaustive list is simply to illustrate that 1 g of live plants will commonly have the equivalent hydrogen content of 0.75- 0.8 g water (assuming 60-100 wt% water content range), and dead plant matter does not lag far behind (0.7 g water equivalent; assuming 40 wt% water content). Due to the long attenuation length for thermal neutrons in air (32 m at sea level; see also sect. 3.3 above) plant matter in the first 10-15 metres above ground will significantly contribute to the enhanced neutron flux in the subsurface and above ground biomass such as duff, grass, plant trunks and branches, can, in principle, have an effect similar to snow-cover.

Many factors can influence the accuracy of above ground biomass estimations such as soil type, soil nutrients, climate, disturbance regime, successional status, topographic position, landscape scale and human impacts (cf. (Mani and Parthasarthy, 2007)). The following overview is therefore only aimed at providing an idea of the magnitudes involved (near natural areas; all values are as DM g/cm^2; DM values are provided in the references; DM values assumed/reconstructed for Plug et al. 2007): Savannah vegetation in semi-arid to arid regions have a relatively low biomass with shrubs at ~0.12 g/cm^2 and grass at ~0.06 g/cm^2 (Patagonia; (Flombaum and Sala, 2007), dry tropical evergreen forests ~1 g/cm^2 (trees only, India; (Mani and Parthasarthy, 2007), neotropical forests 1.5-3 g/cm^2 (Central America; (Drake et al., 2003), Acadian boreal forest ~2 g/cm^2 (trees and branches; Plug et al. 2007); temperate forests 3.3±0.8 g/cm^2 (Central Europe; (Szwagrzyk and Gazda, 2007); and temperate rain forest ~9.5 g/cm^2 (trees and branches; Plug et al. 2007). Estimates for moss cover range between ~0.01 g/cm^2 (Binkley and Graham, 1981) and 0.02-3 g/cm^2 (Gordall et al., 2009; Rieley et al., 1979; Tamm, 1953; Telfer, 1972; Traczyk et al., 1973; Weeman and Timmer, 1967). For mosses it is important to note that they can retain significant amounts of extracellular water; non-saturated extracellular water contents of moss can range widely: e.g. ~10 Vol% (forest floor with *Pleurozium schreberi*; (Price et al., 1997)); or 0-50 Vol% (*Sphagnum capillifolium,* growing as

hummocks; (Hayward and Clymo, 1982). At water saturated conditions the extracellular water content exceeds 90 Vol% (Hayward and Clymo, 1982). Cushion forming moss species in temperate forests have the capacity to intercept and hold ~60 Vol% of precipitation (Moul and Buell, 1955).

The relative mass of downed dead plant matter (e.g. woody debris, litter, and duff) in forests is widely variable, typically ranging between 30 and 60 wt% of the live tree biomass (DM) in temperate/ tropical and moist boreal forest (Gould et al., 2008); in dry boreal areas this value can be as high as >130% (Gould et al., 2008). Assuming a mean of 45 wt% and estimates for tree biomass of 'normal' temperate and boreal forests (2-3.3 g/cm^2; excluding temperate rain forest; (Plug et al., 2007; Szwagrzyk and Gazda, 2007) a downed plant matter cover of 0.9-1.5 g/cm^2 (DM) may be considered as a typical value for these areas. Duff and litter in temperate woodlands can hold as much as ~260 wt% water (relative to DM; pine and oak woodland, New Jersey (Bernard, 1963).

Taking the mass of live and downed plant matter together, it appears that in many areas, particularly temperate and/or humid areas in their natural state (i.e. forested, most of the time), the water equivalent mass of plant matter cover is commonly larger than 2-3 g/cm^2. Consequently in these areas the typical situation might be one of maximum enhancement of the neutron flux in the subsurface, with a ~2.5-fold year-round increase in the thermal neutron flux compared to the not-covered case.

4.2. Effect on calculated production rates

Any snow or plant cover currently considered in cosmogenic nuclides studies is invariably assumed to be a medium which reduces cosmogenic nuclide production (Gosse and Phillips, 2001; Plug et al., 2007), and often a snow/plant cover correction is not applied due to its negligible effect. Our results demonstrate that these assumptions are false for those nuclides where thermal neutrons make significant contributions to the total production rate (^{3}He, ^{36}Cl, ^{41}Ca). Depending on the relative importance of the thermal neutron flux for the total production of a cosmogenic nuclide, actual production rates can be higher by 150% than if calculated without considering a hydrogen-rich cover (Fig. 7). Ignoring this effect could yield exposure ages that are up to 150% to high. Likewise, ratios of nuclides with and without thermal neutron production, e.g. ^{3}He/^{10}Be, (Amidon et al., 2008; Dunai et al., 2007; Gayer et al., 2004; Schimmelpfennig et al., 2011b) would be unexpectedly high when not considering the effect of a hydrogen-rich cover.

In some areas it is probably reasonable to assume the maximum effect (temperate and humid regions, see 4.1) is operating most of the time (permanent hydrogen-rich cover, be it snow or plant

matter, > 2-3 g/cm^2 water equivalent). In other areas that have less and more temporally variable hydrogen-rich cover, such as vegetation in semi-arid regions, or regions with intermittent snow cover, the effect will be difficult to correct for given the temporal and/or spatial range of correction factors will vary between 0 and ~2.5. It is probably only in arid environments, with negligible amounts of vegetation and snow cover, where the effect can safely be ignored; although the presence of gypsum, which contains water, may complicate this situation.

With some developmental work the effect of hydrogen-rich covers on thermal neutron production pathways may be used to extract qualitative information about the long-term average plant/snow cover on stable surfaces. Differences observed in the cosmogenic nuclide concentrations of pairs of target minerals, one whose cosmogenic nuclide production is dominated by the thermal neutron pathway the other dominated by spallation, would reveal minimum average thicknesses of cover over the timescales relevant to cosmogenic nuclide systematics. Previously it has been suggested that such pairs could be used to assess past soil moisture and snow pack thickness (Desilets et al., 2010). Potential targets for such a strategy could be Cl-rich micas for ^{36}Cl, which would be dominated by thermal neutron production, and Cl-poor feldspar for ^{36}Cl, which would be dominated by spallogenic production. An alternative 'paleomoisture recorder' could be ^{36}Cl and ^{41}Ca in Cl-poor plagioclase, the former providing the spallogenic production rate, the latter the pure thermal production (Dunai, 2010). The ^{36}Cl/^{41}Ca ratio in such material would be a measure of the time-integrated effect of a hydrogen-rich cover on rock surfaces. The production rate ratios obtained from such pairs could indicate the presence or absence of hydrogen-rich cover in the past, which may be different to the present day situation due to, for example, aridification and/or warming.

5. Conclusions

Hydrogen-rich covers, such as snow or biomass, increase the thermal neutron flux in an underlying rock surface significantly. The rock serves as the main source for thermal neutrons, the hydrogen-rich cover as a neutron reflector. 2-3 cm water equivalent cover, which would be negligible in terms of moderating the high-energy neutron flux (>10 MeV), provides the maximum enhancement of the thermal neutron flux (>2.5 fold increase). This increase is made up from three components: (1) reflected thermal neutrons (albedo neutrons), (2) moderated fast neutrons from the ground, and (3) moderated fast neutrons from the atmospheric cascade (Masarik et al., 2007). The thermal neutron flux is enhanced to a depth of about 3 diffusion path lengths below the rock surface (24 g/cm^2 in

granite, Liu et al. 1994). In temperate/humid environments it can be expected that the maximum effect is operating in many situations.

The higher thermal neutron flux increases the production rates of cosmogenic nuclides with a significant thermal neutron production pathway (^{3}He, ^{36}Cl, ^{41}Ca), provided the corresponding target nuclei are available (^{6}Li, ^{35}Cl, ^{40}Ca). Ignoring the effect in situations where a significant hydrogen-rich cover has been present will severely underestimate production rates. Corrections for the effect may have significant uncertainties (estimated at ±20% for the correction, *not* the total production rate). However, not correcting for this effect introduces order of magnitude larger errors. For accurate exposure ages using ^{3}He, ^{36}Cl, and ^{41}Ca, it is prudent to select target minerals that are poor in ^{6}Li, ^{35}Cl, ^{40}Ca, respectively (Dunai, 2010; Dunai et al., 2007; Marrero, 2012; Schimmelpfennig et al., 2009; Schimmelpfennig et al., 2011a).

The increase in thermal neutron flux due to hydrogen-rich ground cover has the potential to be used for studies that are aimed at reconstructing the persistence of past plant or snow cover. Isotopic ratios of spallogenic and dominantly thermal neutron produced nuclides could reveal the presence or absence of a hydrogen-rich cover in the past, which may be different to the present day situation.

Acknowledgements

We would like to thank David Sanderson (SUERC), David Thomas and Peter Kolokowski (both NPL) for providing access to neutron sources and helping with the initial set up of the data loggers; Mehmet Karatay and Fin Stuart for helping with the backbreaking building and removing of the granite piles at the airfield; the MOD for providing access to the Kirknewton Airfield and Sqn Ldr Allan J Gillespie for being a patient host for the long-standing granite piles. The study was funded as part of CRONUS-EU by the 6th Framework program of the European Commission, under contract MC-RTN-511927.

Figure captions:

Figure 1: Sketch of the principal dimensions of the two granite piles in oblique and top view. The core-drilled granite blocks that held the neutron counting tubes are shown; the other blocks are not shown individually but had the same dimensions 5 x 10 x 20 cm, only without hole. In the oblique view the position of the additional granite blocks put on top of one of the pile, to mimic a depth profile, is shown in stippled outline. In the top view the centred positions of the water basin and PE sheets are indicated, as is the limit of thrice the thermal neutron diffusion length around the active length of the tube.

Figure 2: Positions of the two granite piles 1 and 2 on the tarmac of an abandoned runway of the MOD's Kirknewton Airfield, Scotland, UK.

Figure 3: Neutron detector count rates as a function of the distance to the eastern edge of pile 2. The neutron detector tubes were moved from the centre position (60 cm) in 10 cm steps towards the edge. Due to the fact that the neutron tube was located in the centre of the granite blocks (see Fig. 1) experiments could not be performed at the very edge of the pile (0 cm). In both experiments, with and without 2 cm PE cover, the linear arrays of count rates at 30, 20, and 10 cm indicate that an extrapolation to 0 cm is permissible. At the centre position (0 cm) five repeat measurements were conducted without cover and a triplet with 2 cm PE cover. The scatter in five repeat measurements without cover provides our estimate for the reproducibility of measurements (±3%; ±1σ), these measurements were conducted over a period of three weeks. Error bars indicate ±1σ. Discussion is provided in the text.

Figure 4: Schematic sketch of the count rate enhancement in a thermal neutron counting tube by moderated fast evaporation neutrons in a neutron reflector. Fast neutrons emitted at a shallow angle to the surface would be lost without a neutron reflector. Thus such shallow emitted fast neutrons may contribute to the count rate in situations with a neutron reflector, provided the evaporating nuclei are within ~1.5 m of the counting tube. In situations with non-infinite surfaces, lateral truncation of the surface will decrease the counting rate, since part of the source of these fast evaporation neutrons, namely the ground beneath the surface, is removed. Further discussion is provided in the text.

Figure 5: Thermal neutron flux in granite as a function of depth below surface. Error bars indicate ±1σ. For this experiment additional granite blocks were placed in 5 cm thick layers on top of pile 2. Calculated depth-dependent fluxes for the actual granite composition (Table 1) are indicated as solid (Schimmelpfennig et al., 2009) and stippled (Phillips and Plummer, 1996) lines. The neutron fluxes are normalized to the count rate without additional granite cover for the experiments, and to 0 cm depth for the calculated curves. Discussion is provided in the text.

Figure 6: Neutron detector counting rates as function of thickness of water equivalent cover placed on top of them. Green diamonds indicate the rates of our ^{3}He-counting tube in granite covered by PE-sheets of variable thicknesses, the pink diamond indicates the experiment where air-gaps were between the PE sheets. Blue circles indicate the corresponding rates obtained in experiments with water. Vertical error bars indicate ±1σ, horizontal error bars the range in water level measured at the beginning and the end of the water experiments. For comparison, the neutron detector counting rates of an experimental MN64 monitor (Hatton and Carmichael, 1964) are shown (white and grey triangles pointing up). The PE cover used in these experiments was converted into water equivalent cover in the same manner as for our experiments (see text). The rates of the BF_3-counting tubes in the MN64 monitor respond very similarly to our experiments to water equivalent cover. Both ^{3}He- and BF_3-conting tubes record thermal neutrons (Clem and Dorman, 2000). The results of a model simulation (Masarik et al., 2007) is indicated by the yellow triangle pointing down. Discussion is provided in the text.

Figure 7: The increase of the production rate as function of the relative contribution of thermal neutrons to cosmogenic nuclide production rates (dashed line), for situations with a factor 2.5 enhancement of the thermal neutron flux in a surface below a hydrogen-rich cover. The increase is relative to the situation without a hydrogen-rich cover. Also shown is the estimated uncertainty of the corresponding production rates (corrected for the effects of a hydrogen-rich cover), assuming a 20% uncertainty of the correction (solid line). For the calculation of both curves, a permanent hydrogen-rich cover of > 2 cm water equivalent was assumed. Note, that while the correction might have a considerable uncertainty, ignoring the effect of a neutron reflector results in a potential error one order of magnitude larger (y-axes are logarithmic).

Table 1:

	SiO_2	Al_2O_3	Fe_2O_3	MnO	MgO	CaO	Na_2O	K_2O	TiO_2	P_2O_5	LOI	H-Total
Granite	71.11	14.55	2.24	0.062	0.51	2.48	3.84	3.37	0.236	0.08	0.53	0.03
Tarmac	49.94	13.00	12.86	0.188	4.34	6.83	3.42	1.23	2.507	0.4	5.6	0.54

Major element concentrations of the granite used to build the piles and of the tarmac on which the piles stood, concentrations are in wt.%. Trace element concentrations in the granite are: Sm: 2.58 ppm, Gd: 1.9 ppm, Th: 8.81 ppm, U: 2.57 ppm, B: 10.2 ppm, Li: 26 ppm. Hydrogen content was determined by pyrolysis and IR-analysis of water evolved. Analyses conducted by Actlabs (www.actlabs.com).

References:

Amidon, W.H., Farley, K.A., Burbank, D.W., Pratt-Sittaula, B., 2008. Anomalous cosmogenic ^{3}He production and elevation scaling in the high Himalaya. Earth and Planetary Science Letters 265, 287-301.

Audi, G., Bersillon, O., Blachot, J., Wapstra, A.H., 2003. The NUBASE evaluation of nuclear and decay properties. Nuclear Physics A 729, 3-128.

Bernard, J.M., 1963. Forest floor moisture capacity of the New Jersey Pine Barrens. Ecology 44, 574-576.

Binkley, D., Graham, R.L., 1981. Biomass, production, and nutrient cycling of mosses in an old-growth douglas-fir forest. Ecology 62, 1387-1389.

Chadwick, M.B., Obložinský, P., Herman, M., Greene, N.M., McKnight, R.D., Smith, D.L., Young, P.G., MacFarlane, R.E., Hale, G.M., Frankle, S.C., Kahler, A.C., Kawano, T., Little, R.C., Madland, D.G., Moller, P., Mosteller, R.D., Page, P.R., Talou, P., Trellue, H., White, M.C., Wilson, W.B., Arcilla, R., Dunford, C.L., Mughabghab, S.F., Pritychenko, B., Rochman, D., Sonzogni, A.A., Lubitz, C.R., T.H., T., Weinman, J.P., Brown, D.A., Cullen, D.E., Heinrichs, D.P., McNabb, D.P., Derrien, H., Dunn, M.E., Larson, N.M., Leal, L.C., Carlson, A.D., Block, R.C., Briggs, J.P., Cheng, E.T., Huria, H.C., Zerkle, M.L., Kozier, K.S., Courcelle, A., Pronyaev, V., van der Marck, S.C., 2006. ENDF/B-VII.0: Next Generation Evaluated Nuclear Data Library for Nuclear Science and Technology. Nuclear Data Sheets 107, 2931-3060.

Clem, J.M., Dorman, L.I., 2000. Neutron monitor response functions. Space Science Reviews 93, 335-359.

Csikai, J., Buczkó, C.M., 1998. The concept of the reflection cross section of thermal neutrons. Applied Radiation and Isotopes 50, 487-490.

Desilets, D., Zreda, M., Ferre, T.P.A., 2010. Nature's neutron probe: Land surface hydrology at an elusive scale with cosmic rays. Water Resources Research 46.

Dilks, T.J.K., Proctor, M.C.F., 1979. Photosynthesis, respiration and water content in bryophytes. New Phytol. 82, 97-114.

Dinwoodie, J.M., 2000. Timber: Its Nature and Behaviour. Spon Press, London.

Drake, J.B., Knox, R.G., Dubayah, R.O., Clark, D.B., Condit, R., Blair, J.B., Hofton, M., 2003. Above-ground biomass estimation in closed canopy Neotropical forests using lidar remote sensing: factors affecting the generality of relationships. Global Ecology & Biogeography 12, 147-159.

Dunai, T.J., 2010. Cosmogenic nuclides: principles, concepts and applications in the Earth surface sciences. Cambridge University Press, Cambridge.

Dunai, T.J., Stuart, F.M., Pik, R., Burnard, P.G., Gayer, E., 2007. Production of ^{3}He in crustal rocks by cosmogenic thermal neutrons. Earth Planet. Sci. Lett. 258, 228-236.

Farley, K.A., Libarkin, J., Mukhopadhyay, S., Amidon, W., 2006. Cosmogenic and nucleogenic ^{3}He in apatite, titanite, and zircon. Earth Planet. Sci. Lett. 248, 451-461.

Flombaum, P., Sala, O.E., 2007. A non-destructive and rapid method to estimate biomass and aboveground net primary production in arid environments. Journal of Arid Environments 69, 353-358.

Gayer, E., Pik, R., Lavé, J., France-Lanord, C., Bourlès, D., Marty, B., 2004. Cosmogenic ^{3}He in Himalayan garnets indicating an altitude dependence of the ^{3}He/^{10}Be production ratio. Earth Planet. Sci. Lett. 229, 91-104.

Goldhagen, P., Clem, J.M., Wilson, J.W., 2003. Recent results from measurements of the energy spectrum of cosmic-ray induced neutrons aboard an ER-2 airplane and on the ground. Adv. Space. Res. 32, 35-40.

Goldhagen, P., Reginatto, M., Kniss, T., Wilson, J.W., Singleterry, R.C., Jones, I.W., W., V.S., 2002. Measurement of the energy spectrum ofcosmic-ray induced neutrons aboard an ER-2 high-altitude airplane. Nuclear Instruments and Methods in Physics Research A 476, 42-51.
Gordall, J.L., Wooding, S.J., Jónsdóttir, I.S., Van der Waal, R., 2009. Herbivore impacts to the moss layer determine tundra ecosystem response to grazing and warming. Ecosystem Ecology 161, 747-758.
Gosse, J.C., Phillips, F.M., 2001. Terrestrial in situ cosmogenic nuclides: theory and application. Quat. Sci. Rev. 20, 1475-1560.
Gould, W.A., Gonzalez, G., Hudak, A.T., Nettleton Hollingsworth, T., Hollingsworth, J., 2008. Forest Structure and Downed Woody Debris in Boreal, Temperate, and Tropical Forest Fragments. Ambio 37, 577-587.
Hatton, C.J., Carmichael, H., 1964. Experimental investigation of NM-64 neutron monitor. Canadian Journal of Physics 42, 2443-2472.
Hayward, P.M., Clymo, R.S., 1982. Profiles of water content and pore size in Sphagnum and peat, and their relation to peat bog ecology. Proc. R. Soc. Lond. B 215, 299-325.
Hendrick, L.D., Edge, R.D., 1966. Cosmic-ray neutrons near Earth. Phys. Rev. 145, 1023-1025.
Hooper, A.W., 1980. Estimation of the moisture content of grass from diffuse reflectance measurements at near infrared wavelengths. Journal of Agricultural Engineering research 25, 355-366.
Kastner, J., Oltman, B.G., Feige, Y., Gold, R., Congel, F., 1970. Nuclear radiation detection for the natural environment. IEEE Transactions on Nuclear Science NS17, 144-150.
Király, B., Csikai, J., 2000. Investigations on thermal neutron reflection by activation method. Applied Radiation and Isotopes 52, 93-96.
Kodama, M., 1980. Continous monitoring of snow water equivalent using cosmic ray neutrons. Cold region Sci. Technol. 3, 295-303.
Kodama, M., 1983. Ground albedo neutrons produced by Cosmic Radiations. J. Phys. Soc. Japan 52, 1503-1504.
Kodama, M., Kudo, S., Kosuge, T., 1985. Application of atmospheric neutrons to soil moisture measurement. Soil Science 140, 237-242.
Kowatari, M., Nagaoka, K., Satoh, S., Ohta, Y., Abukawa, J., Tachimori, S., Nakamura, T., 2005. Evaluation of the Altitude Variation of the Cosmic-ray induced Environmental Neutrons in the Mt.Fuji Area. Journal of Nuclear Science and Technology 42, 495-502.
Lal, D., Peters, B., 1967. Cosmic ray produced radioactivity on earth, in: Flugg, S. (Ed.), Handbook of Physics. Springer, Berlin, pp. 551-612.
Liu, B., Phillips, F.M., Fabryka-Martin, J.T., Fowler, M.M., Stone, W.D., 1994. Cosmogenic ^{36}Cl accumulation in unstable landforms: 1. Effects of the thermal neutron distribution. Water Resour. Res. 30, 3115-3125.
Mani, S., Parthasarthy, N., 2007. Above-ground biomass estimation in ten tropical dry evergreen forest sites of peninsular India. Biomass and Bioenergy 31, 284-290.
Marrero, S.M., 2012. Calibration of cosmogenic chlorine-36. New Mexico Institute of Mining and Technology, Socorro, p. 365.
Masarik, J., Kim, K.J., Reedy, R.C., 2007. Numerical simulations of in situ production of terrestrial cosmogenic nuclides. Nucl. Inst. Meth. Phys. Res. B 259, 642-645.
Moul, E.T., Buell, M.F., 1955. Moss cover and rainfall interception in frequently burned sites in the New Jersey Pine Barrens. Bulletin of the Torrey Botanical Club 82, 155-162.
Nishiizumi, K., Caffee, M.W., DePaolo, D.J., 2000. Preparation of ^{41}Ca AMS standards. Nucl. Instr. Meth. Phys. Res. B 172, 399-403.
O'Brien, K., Sandmeier, H.A., Hansen, G.E., 1978. Cosmic ray induced neutron background sources and fluxes for geometries of air over water, ground, iron and aluminium. Journal of Geophysical Research 83, 114-120.

Onuchin, A.A., Burenina, T.A., 1996. Climatic and geographic patterns in snow density dynamics, Northern Eurasia. Arctic and Alpine Research 28, 99-103.
Phillips, F.M., Plummer, M.A., 1996. CHLOE: A program for interpreting in-situ cosmogenic nuclide data for surface exposure dating and erosion studies. Radiocarbon 38, 98-99.
Phillips, F.M., Stone, W.D., Fabryka-Martin, J.T., 2001. An improved approach to calculating low-energy cosmic ray neutron fluxes near the land/atmosphere interface. Chem. Geol. 175, 689-701.
Plug, L.J., Gosse, J., McIntosh, J.J., Bigley, R., 2007. Attenuation of cosmic ray flux in temperate forest. Journal of Geophysical Research - Earth Surface 112, F02022.
Price, A.G., Dunham, K., Carleton, T., Band, L., 1997. Variability of water fluxes through the black spruce (Picea mariana) canopy and feather moss (Pleurozium schreberi) carpet in the boreal forest of Northern Manitoba. Journal of Hydrology 196, 310-323.
Reuss, P., 2008. Neutron Physics. EDP Sciences, Les Ulis.
Rieley, J.O., Richards, P.W., Bebbington, A.D.L., 1979. The ecological role of bryophytes in a North Wales woodland. Journal of Ecology 67, 497-527.
Robichaud, P.R., Gasvoda, D.S., Hungerford, R.D., Bilskie, J., Ashmun, L.E., Reardon, J., 2004. Measuring duff moisture content in the field using a portable meter sensitive to dielectric permittivity. International Journal ofWildland Fire 13, 343-353.
Schimmelpfennig, I., Benedetti, L., Finkel, R.C., Pik, R., Blard, P.H., Bourlès, D., Burnard, P.G., Williams, A.J., 2009. Sources of in-situ 36Cl in basaltic rocks. Implications for calibration of production rates. Quaternary Geochronology, doi:10.1016/j.quageo.2009.1004.1003.
Schimmelpfennig, I., Benedetti, L., Garreta, V., Pik, R., Blard, P.H., Burnard, P., Bourles, D., Finkel, R., Ammon, K., Dunai, T., 2011a. Calibration of cosmogenic (36)Cl production rates from Ca and K spallation in lava flows from Mt. Etna (38 degrees N, Italy) and Payun Matru (36 degrees S, Argentina). Geochimica et Cosmochimica Acta 75, 2611-2632.
Schimmelpfennig, I., Williams, A., Pik, R., Burnard, P., Niedermann, S., Finkel, R., Schneider, B., Benedetti, L., 2011b. Inter-comparison of cosmogenic in-situ He-3, Ne-21 and Cl-36 at low latitude along an altitude transect on the SE slope of Kilimanjaro volcano (3 degrees S, Tanzania). Quaternary Geochronology 6, 425-436.
Szwagrzyk, J., Gazda, A., 2007. Above-ground standing biomass and tree species diversity in natural stands of Central Europe. Journal of Vegetation Science 18, 555-562.
Tamm, C.O., 1953. Growth, yield and nutrition in carpets of a forest moss (Hylocominum spendens). Meddelanden fran Statens Skogsförskingsinstitut 43, 1-140.
Telfer, E.S., 1972. Understory biomass in five forest types in southwestern Nove Scotia. Canadian Journal of Botany 50, 1263-1267.
Thomas, D.J., Kolokowski, P., 2005. Thermal fluence and dose equivalent standards at NPL. NPL Report DQL-RN 008.
Traczyk, T., Traczyk, H., Moszynska, B., 1973. Herb layer production of 2 pinewood communities in teh Kampinos National Park. Ekologia Polska 21, 37-55.
Vega-Carillo, H.R., Manzanares-Acuna, E., Hernandes-Davila, V.M., Sanchez, G.A.M., 2005. Response matrix of a multisphere neutron spectrometer with an He-3 proportional counter. Revista Mexicana de Fisica 51, 47-52.
Weeman, G.G., Timmer, V., 1967. Feather moss growth and nutrient content under upland black spruce. Pulp and Paper Canada, Technical Report 503, 1-38.
Yamashita, M., Stephens, L.D., Patterson, H.W., 1966. Cosmic-ray-produced neutrons at ground level: neutron production rate and flux distribution. J. Geophys. Res. 71, 3817-3834.
Zreda, M., Desilets, D., Ferré, T.P.A., Scott, R.L., 2008. Measuring soil moisture content non-invasively at intermediate spatial scale using cosmic-ray neutrons. Geophys. Res. Lett. 35, L21402.

Figure 1.

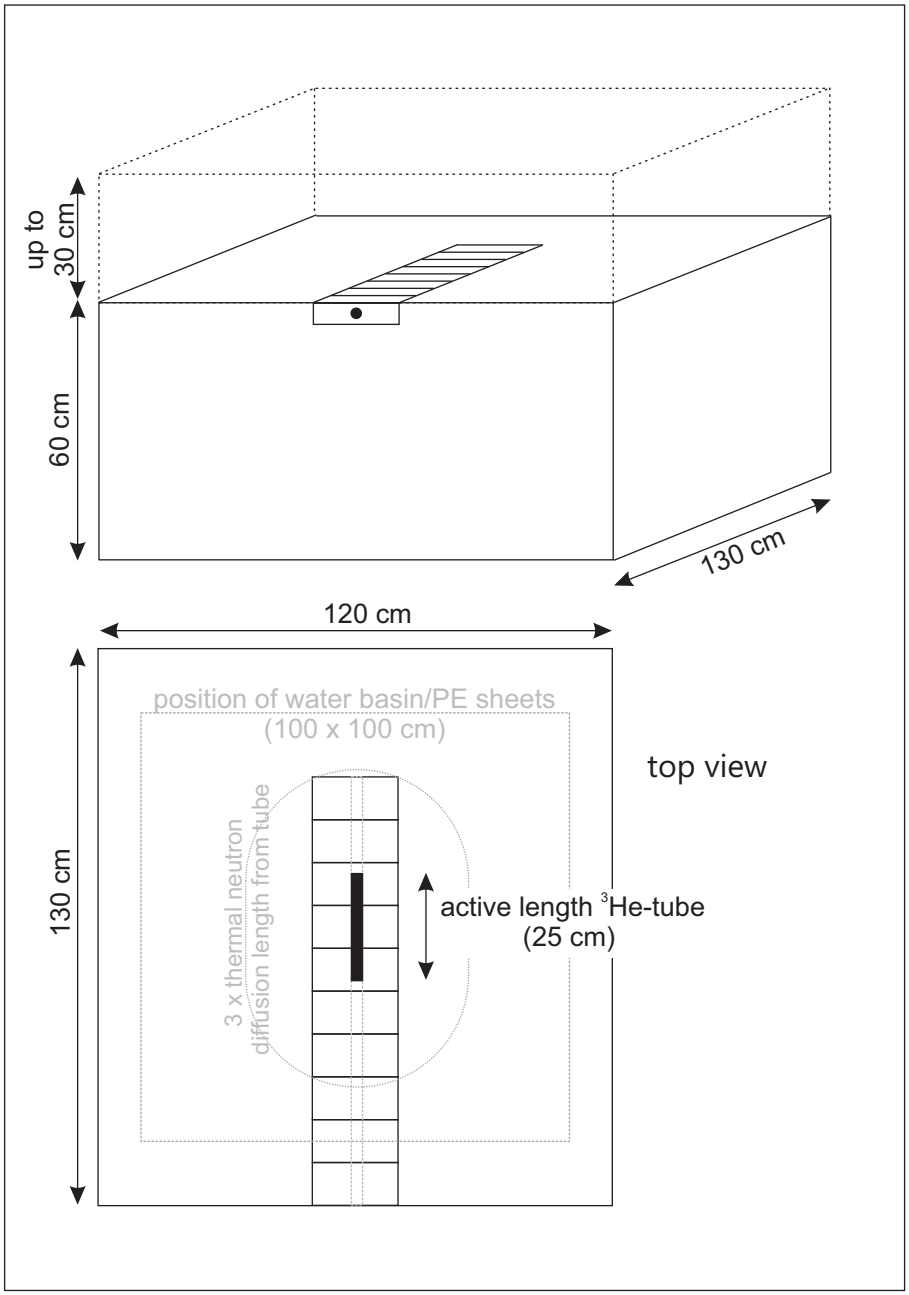
up to 30 cm
60 cm
130 cm
120 cm
130 cm
position of water basin/PE sheets
(100 x 100 cm)
top view
3 x thermal neutron diffusion length from tube
active length ^{3}He-tube
(25 cm)

Figure 2.

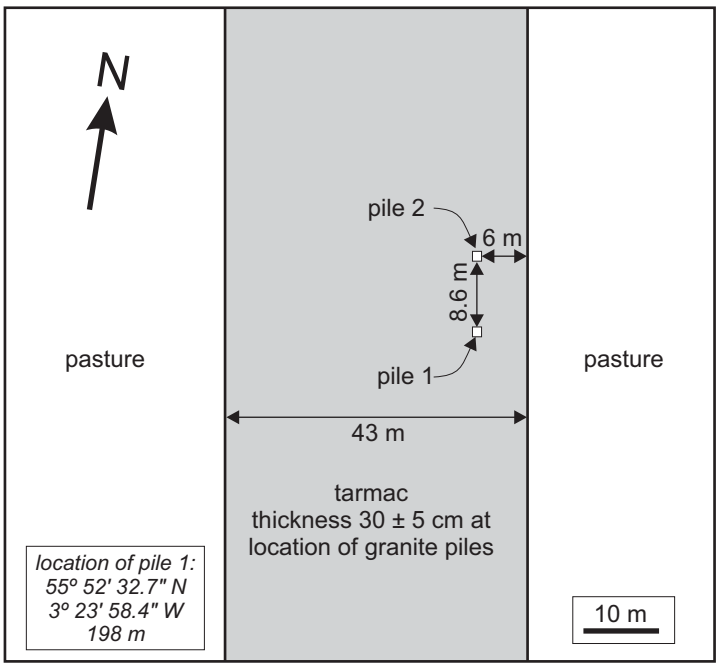
N
pile 2
6 m
8.6 m
pile 1
pasture
pasture
43 m
tarmac
thickness 30 ± 5 cm at
location of granite piles
location of pile 1:
55º 52′ 32.7″ N
3º 23′ 58.4″ W
198 m
10 m

Figure 3.

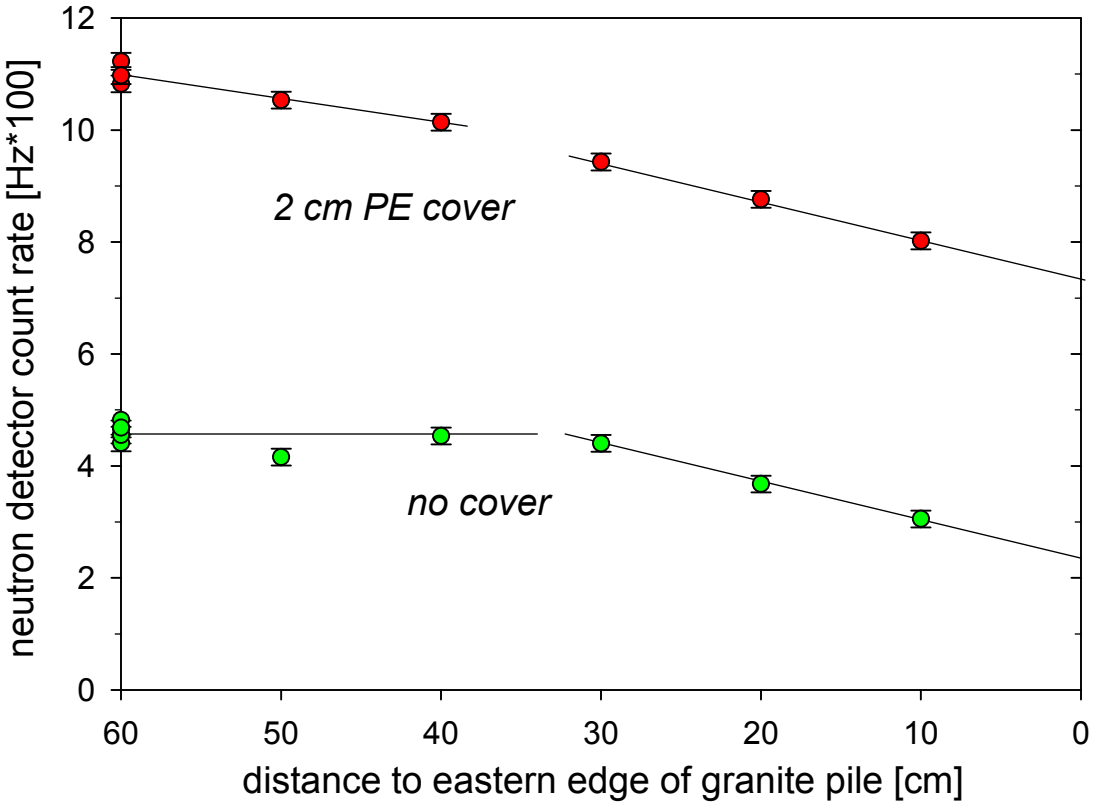
neutron detector count rate [Hz*100]
distance to eastern edge of granite pile [cm]
2 cm PE cover
no cover
0
2
4
6
8
10
12
60
50
40
30
20
10
0

Figure 4.

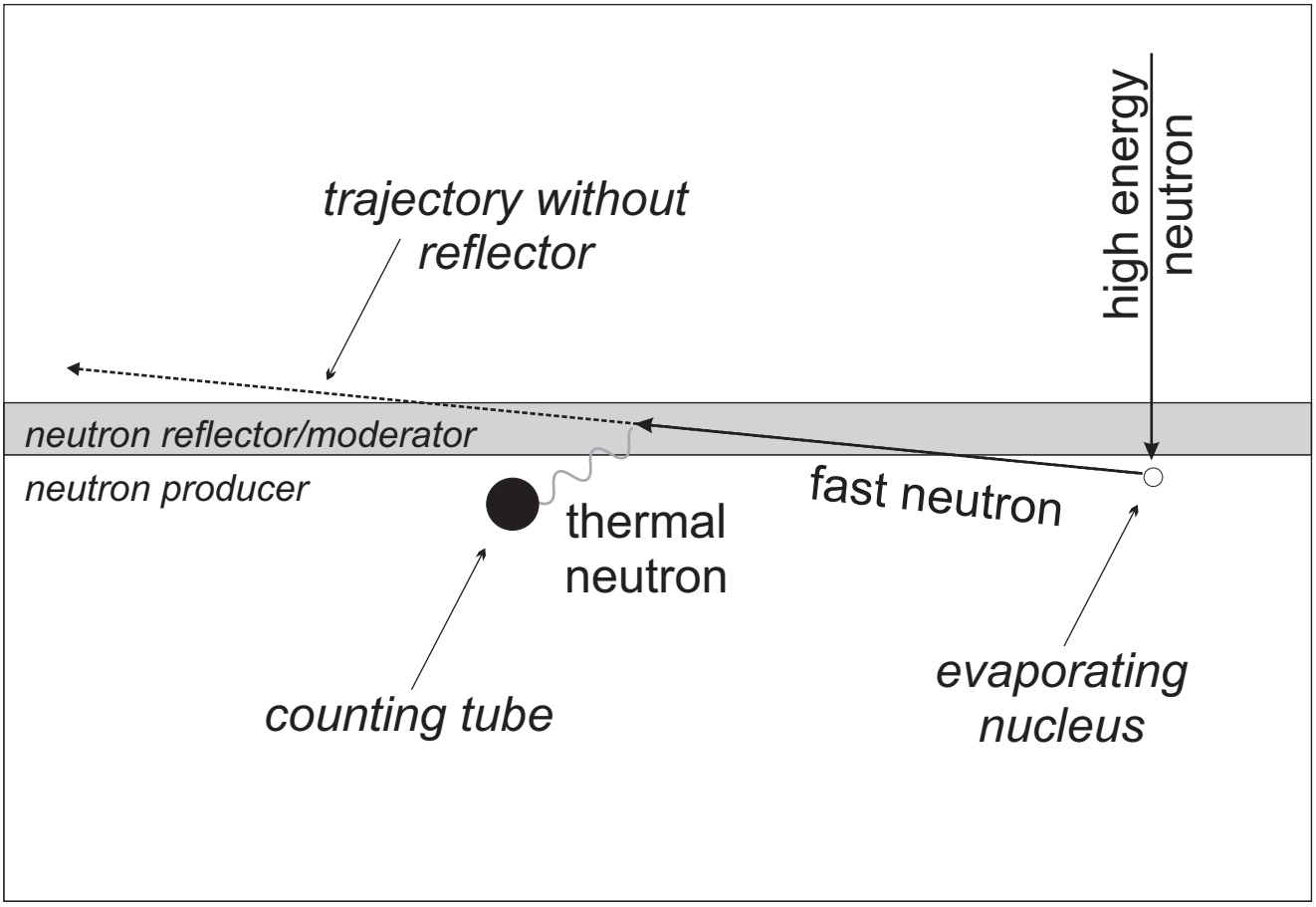
high energy neutron
trajectory without reflector
neutron reflector/moderator
neutron producer
fast neutron
thermal neutron
counting tube
evaporating nucleus

Figure 5.

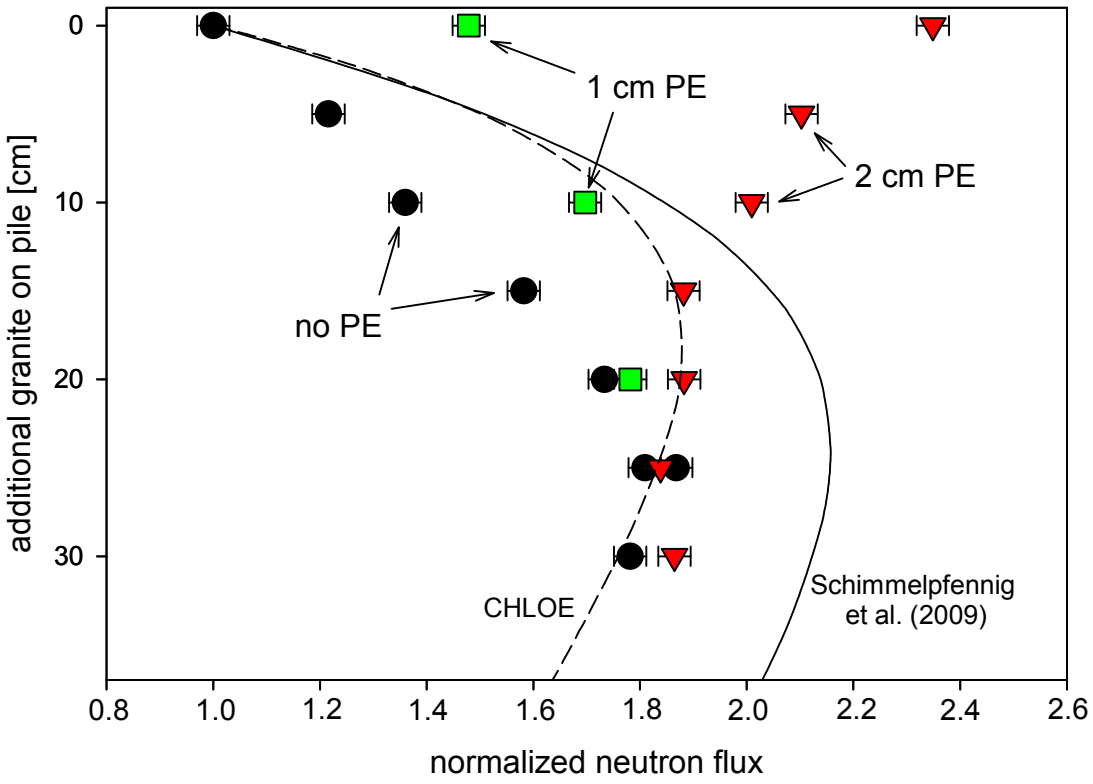
0
10
20
30
additional granite on pile [cm]
1 cm PE
2 cm PE
no PE
CHLOE
Schimmelpfennig
et al. (2009)
0.8
1.0
1.2
1.4
1.6
1.8
2.0
2.2
2.4
2.6
normalized neutron flux

Figure 6.

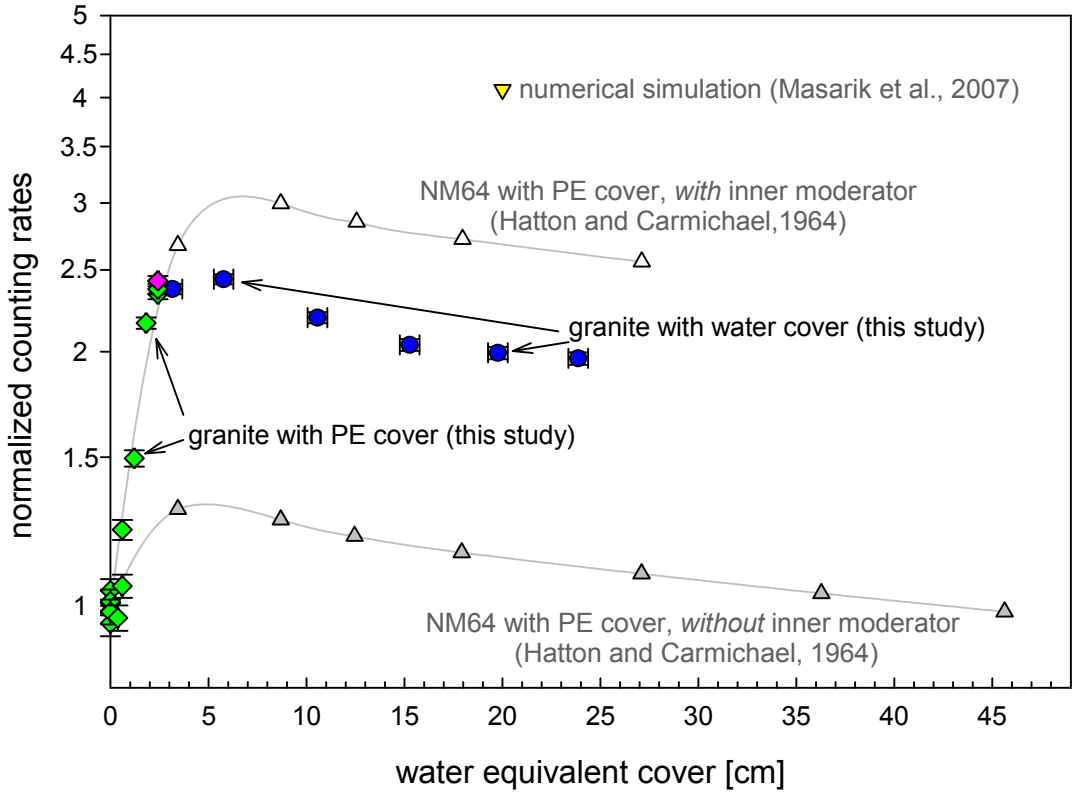
numerical simulation (Masarik et al., 2007)
NM64 with PE cover, *with* inner moderator
(Hatton and Carmichael,1964)
granite with water cover (this study)
granite with PE cover (this study)
NM64 with PE cover, *without* inner moderator
(Hatton and Carmichael, 1964)
normalized counting rates
water equivalent cover [cm]
5
4.5
4
3.5
3
2.5
2
1.5
1
0
5
10
15
20
25
30
35
40
45

Figure 7.

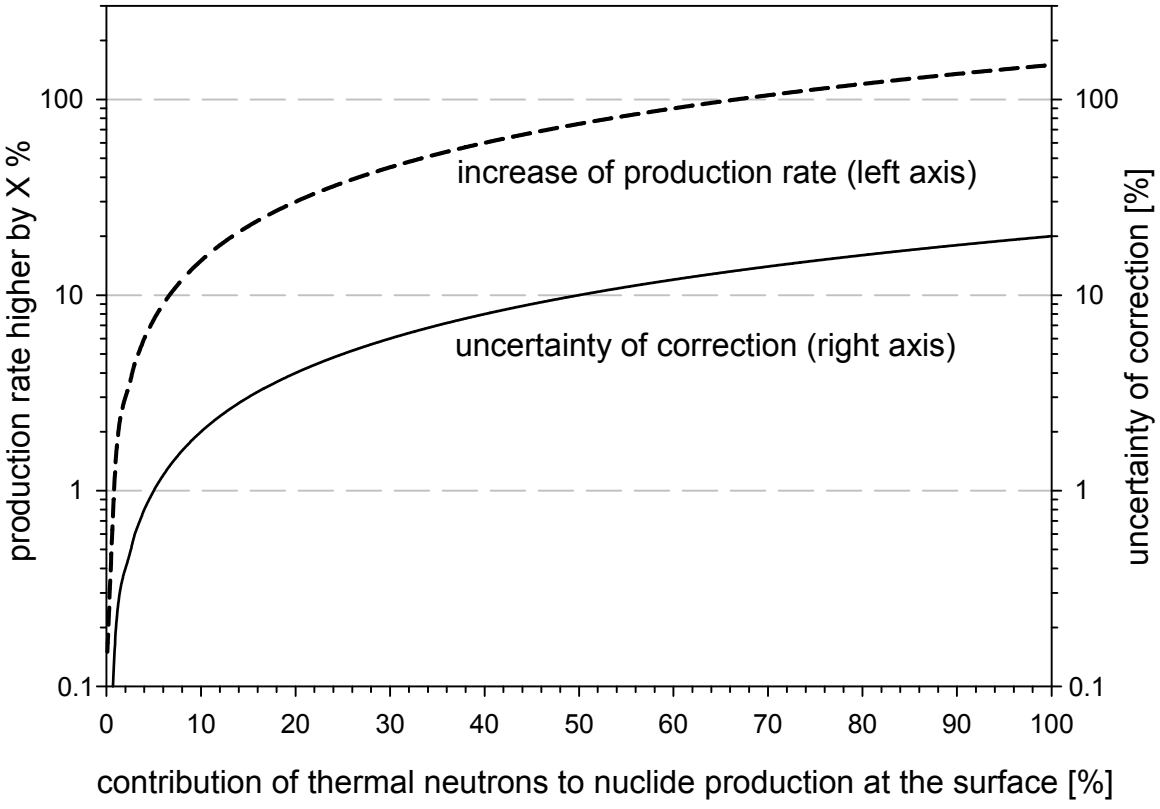
production rate higher by X %
uncertainty of correction [%]
increase of production rate (left axis)
uncertainty of correction (right axis)
100
10
1
0.1
0
10
20
30
40
50
60
70
80
90
100
contribution of thermal neutrons to nuclide production at the surface [%]